International Journal of Pharmaceutics 532 (2017) 660–668

Contents lists available at ScienceDirect

International Journal of Pharmaceutics

journal homepage: www.elsevier.com/locate/ijpharm

Stealth magnetic nanocarriers of siRNA as platform for breast cancer theranostics

J. Bruniaux, S. Ben Djemaa, K. Hervé-Aubert, H. Marchais, I. Chourpa, S. David*

Université François-Rabelais, EA6295 « Nanomédicaments et Nanosondes », Tours, 37200, France

ARTICLE INFO

Article history:
Received 20 January 2017
Received in revised form 9 May 2017
Accepted 10 May 2017
Available online 12 May 2017

Keywords:
Chitosan
Poly-L-arginine
siRNA
SPION
Transfection

ABSTRACT

The endogenous mechanism of RNA interference is more and more used in research to obtain specific down-regulation of gene expression in diseases such as breast cancer. Currently, despite the new fields of study open up by RNA interference, the rapid degradation of siRNA by nucleases and their negative charges prevent them from crossing cell membranes. To overcome these limitations, superparamagnetic iron oxide nanoparticles (SPIONs) represent a promising alternative for nucleic acid delivery. Previously, we reported the magnetic siRNA nanovectors (MSN) formulation using electrostatic assembly of (1) SPIONs, also able to act as contrast agents for magnetic resonance imaging (MRI), (2) siRNA and (3) chitosan aiming at their protection and enhancing their transfection efficacy. However, these nanoparticles displayed low stability in biological suspensions and inefficient transfection of active siRNA.

This work aimed at upgrading MSN to Stealth MSN (S-MSN) by adding a polyethylene glycol coating to ensure colloidal stability and stealth properties. Furthermore, another polymer (poly-L-arginine) was added for efficient siRNA transfection and the quantitative composition of the formulation was adapted for biological purposes. Results showed that S-MSN provide high siRNA complexation and protection against enzymatic degradation. Green fluorescent protein (GFP) specific down-regulation on MDA-MB231/GFP cells was comparable to that of commercially available reagents, without observable cytotoxicity. According to our works, S-MSN appears as an effective formulation for *in vitro* siRNA specific delivery.

1. Introduction

Breast cancer is the leading cause of mortality in women worldwide, and the second most common cancer overall (Ferlay et al., 2015). In recent years, significant progress has been made in the development of diagnostic tools and surgical treatments. However, treatment of resistant and recurrent metastatic breast cancers still needs a substantive improvement (Kennecke et al., 2010). Actually, about 80 genetic mutations can be identified in an individual breast tumor, including a dozen that are considered to be actively driving oncogenesis (Schlabach et al., 2008; Wood et al., 2007; Zhang et al., 2014). A unique individual profile of gene mutations may be established for each patient allowing a personalized treatment that takes advantage of the high specificity of small interfering RNA (siRNA). These siRNA are able to down-regulate genes responsible for tumorigenesis, including those driving oncogenesis, proliferation, angiogenesis, metastasis and resistance to treatment (Resnier et al., 2013).

siRNA are double-stranded RNA molecules composed of 19-24 pairs of nucleotides that naturally take part in an endogenous post-transcriptional inhibition mechanism used to regulate gene expression: RNA interference (RNAi) (Fire et al., 1998). siRNA interact with a cytosolic RNA-induced silencing complex (RISC) that recognizes a targeted complementary mRNA with high specificity. This action leads to the inhibition of gene expression through mRNA degradation or hindrance in ribosome activity (Meister and Tuschl, 2004).

However, siRNA have a poor ability to cross plasma membranes and reach RNAi intracellular sites of action. siRNA transfection to

Abbreviations: CR_{CS}, charge ratio (chitosan/siRNA); CR_{PS}, charge ratio (poly-L-arginine/siRNA); DLS, dynamic light scattering; GFP, green fluorescent protein; MR, mass ratio (iron content of SPIONs/siRNA); MRI, magnetic resonance imaging; $NaNO_3$, sodium nitrate; PEG, polyethylene glycol; PLR, poly-L-arginine; RISC, RNA induced silencing complex; SFP, stealth fluorescent particles; (S-)MSN, (stealth) magnetic siRNA nanovectors; SPIONs, superparamagnetic iron oxide nanoparticles.

* Corresponding author at: EA 6295 Nanomédicaments et Nanosondes, Laboratoire de pharmacie galénique, Faculté de pharmacie, 31 avenue Monge, 37200 Tours, France.
E-mail address: stephanie.david@univ-tours.fr (S. David).

http://dx.doi.org/10.1016/j.ijpharm.2017.05.022
0378-5173/

cells is limited by their physico-chemical properties: molecular weight and anionic charge restrain considerably their transport across the plasma membrane (De Fougerolles and Novobrantseva, 2008; Juliano et al., 2008; Layzer et al., 2004; Santel et al., 2006). Moreover, siRNA are relatively vulnerable due to degradation by nucleases and their biodistribution after intravenous injection does not allow targeting cancer cells and/or tumors. To overcome these limitations, different strategies have been developed, including the use of delivery systems (Ozcan et al., 2015; Urban-Klein et al., 2005; Yu et al., 2012).

Among delivery systems developed in the last 10 years, nanocarriers based on superparamagnetic iron oxide nanoparticles (SPIONs) appear to be a promising tool (Medarova et al., 2007; Veiseh et al., 2010). Composed of magnetite and maghemite, SPIONs are superparamagnetic: they are highly magnetized in a magnetic field, but lose their magnetization when the field is switched off. SPIONs provide enhanced negative contrast in magnetic resonance imaging (MRI) and their loading with siRNA could allow to combine MRI-mediated diagnostic and therapeutic functions, in a so-called theranostic approach. Anti-cancer theranostic is expected to permit tailored treatment for individual patients, considering the inter-individual variability of therapeutic response.

We have recently described the formulation of magnetic siRNA nanovectors (MSN) (David et al., 2015, 2013) assembled by electrostatic force-stabilized deposition of siRNA (polyanion) and chitosan (polycation) on SPIONs pre-coated with positively charged amino groups. Experimental design approaches were used to optimize physico-chemical properties of MSN (David et al., 2015, 2013). Chitosan is a biodegradable and biocompatible natural polymer consisting of repeating units of D-glucosamine and N-acetyl-D-glucosamine. Chitosan is known to bind negatively charged nucleic acids, enabling this polymer to be used as a gene delivery vehicle (Howard et al., 2006; Techaarpornkul et al., 2010). The nanoparticles developed in our previous work were not stable in culture medium containing fetal bovine serum. The present study aimed at developing a new generation of stealth magnetic siRNA nanovectors (S-MSN). In addition, MSN were also formulated according to the previously described protocols, characterized and used as control samples to be compared with different S-MSN formulations. Compared to MSN, the S-MSN formulation was based on SPIONs labeled with deep red-fluorescent dye sulfocyanine and coated with biocompatible polymer, polyethylene glycol (PEG, MW 5 kDa), both attached covalently. These precursor particles will hereafter be referred to as stealth fluorescent particles (SFP). Moreover, the synthetic cationic polypeptide poly-L-arginine (PLR) (pKa >12) was added in order to compensate the low stability of the siRNA-chitosan complex and to increase transfection efficiency at physiological pH (Lavertu et al., 2006; Mao et al., 2010; Opanasopit et al., 2011). S-MSN formulations were first optimized by adjusting the quantitative composition and characterized to demonstrate their potential for a future administration *in vivo*. Finally, we compared these S-MSN formulations with a commercially available reagent in terms of their siRNA transfection to breast cancer cells, by measuring (i) down-regulation of green fluorescent protein (GFP) expression in MDA-MB231-GFP cells and (ii) cytotoxicity against MDA-MB231 cells.

2. Materials and methods

2.1. Materials

For physico-chemical characterization, model siRNA (targeted against PCSK9, sense sequence GGAAGAUCAUAAUGGACAGdTdT with lower case letters representing deoxyribonucleotides) were provided by Eurogenetec (Angers, France). Poly-L-arginine (MW 15.000-70.000) and high purity chitosan (MW 110.000-150.000; degree of acetylation: ≤40 mol. %), used for MSN and S-MSN formulation, were from Sigma–Aldrich Chemie GmbH (Schnelldorf, Germany). For transfection assay, commercial transfection reagent Oligofectamine® and siRNA were purchased from Life Technologies (Paisley, UK). For gel retardation assays, loading buffer, agarose and ethidium bromide were purchased from Fisher Bioreagents® (Illkirch, France). All the culture media and supplements for cell culture were supplied by life technologies (Paisley, UK).

2.2. MSN and S-MSN preparation

MSN were prepared based on a protocol previously described by David et al. (2015). In contrast to MSN, S-MSN were formulated using SPIONs covalently modified with sulfocyanine fluorescent label and PEG_{5000} polymer (SFP) (Alric et al., 2016; Perillo et al., 2017). Three different formulation protocols were tested: for protocols 1 and 2, siRNA in DPBS 1 × buffer was pre-complexed with an aqueous solution of chitosan or PLR, respectively, before being mixed with SFP suspensions, to obtain S-MSN_1 and S-MSN_2. For protocol 3, siRNA were pre-complexed with PLR, then added to a solution containing SFP and chitosan, to obtain S-MSN_3. The amount of SPIONs (quantified by its iron content) was defined as iron/siRNA mass ratio (MR). For preliminary experiments, the MR was fixed at 10 (David et al., 2015), then optimized with variation from 10 to 70. Chitosan or PLR content was expressed by the charge ratio (CR) of positive polymer charges to negative siRNA charges. For preliminary experiments, the CR of chitosan/siRNA (CR_{CS}) was set to 44 to formulate S-MSN_1 (David et al., 2015), and then adapted with modification from 10 to 100 to obtain optimized S-MSN_3. In the same way, different CR of PLR/siRNA (CR_{PS}) were tested for S-MSN_2 (from 1 to 44) and S-MSN_3 (from 10 to 50).

2.3. Physico-chemical characterization

2.3.1. DLS and zeta potential measurements

The mean hydrodynamic diameter (HD) and zeta potential (ZP) of S-MSN in suspension were determined using a Malvern HPPS instrument (Malvern Instruments, Malvern, UK). Before measurement, the S-MSN preparations were diluted in $NaNO_3$ 0.01 M at a ratio 1:25 to obtain a constant ionic strength (pH = 5.6) (n = 3). The mean values of HD given were based on intensity.

2.3.2. Agarose gel electrophoresis

S-MSN were formulated with a constant final siRNA concentration of 3 μM before addition of water (Milli-Q system, Millipore, Paris, France) or 10 mg/mL heparin sodium used as control (Sigma-Aldrich, Chemie GmbH, Schelldorf, Germany). With its strong negative charge, heparin is used to displace siRNA from its complex prior to electrophoretic analysis of liberated siRNA. Samples were mixed with 1.5 μL loading buffer (Agarose gel loading dye 6X) prior to deposit on 1% agarose gel containing ethidium bromide. A 100 V voltage was applied for about 15 min in a Tris/acetate/EDTA buffer (TAE 1X, 40 mM acetate, EDTA 1 mM, pH 7.6). Gels were visualized and analyzed with EvolutionCapt software on a Fusion-Solo.65.WL imager (Vilbert Lourmat, Marne-la-Vallée, France).

2.3.3. Stability in culture media

S-MSN (20 nM) were added to solution containing equal parts of OptiMEM serum-free medium and Dulbecco's modified Eagle medium (DMEM) supplemented with 10% fetal calf serum to mimic transfection conditions. After 0 to 4 hours incubation, the hydrodynamic diameter was determined by DLS as described in

2.3.1. In parallel, siRNA retention in S-MSN was studied by gel retardation assay as described in 2.3.2.

2.3.4. siRNA protection assay

A S-MSN solution containing 0.4 μg of siRNA was incubated with 2 ng ribonuclease A (Sigma-Aldrich, Chemie GmbH, Schelldorf, Germany) for 2 or 4 hours at 37 °C. Afterwards, ribonuclease A was inactivated by heating the solutions at 70 °C for 30 min. siRNA was released by adding 5 μL of a 10 mg/mL heparin sodium solution and run on agarose gel as described previously. An equivalent amount of free siRNA was used as a positive control to check the ribonuclease A activity.

2.4. Cell culture

Breast cancer cells, MDA-MB231-GFP (Euromedex, Souffelweyersheim, France) and MDA-MB231 (a kind gift from INSERM UMR 1069 Nutrition, Croissance et Cancer (N2C)), were routinely cultured in Dulbecco's modified Eagle medium (DMEM) supplemented with 10% fetal calf serum, non-essential amino acid 1X and 1% penicillin/streptomycin. Cells were maintained at 37 °C in an atmosphere containing 5% CO_2. Culture medium was changed every 48 hours and the cells were harvested using trypsin as soon as 80% confluency was reached.

2.5. siRNA transfection

At 24 h before transfection, 25.10^3 cells/wells were seeded in a 12-well plate containing equal parts OptiMEM serum-free medium and DMEM supplemented with 10% fetal calf serum. Transfections of 20 nM siRNA were carried out by adding a suspension of S-MSN in DPBS representing 8% of final volume.

2.6. Down-regulation efficiency

Transfection was performed on MDA-MB231-GFP cells with anti-GFP siRNA which specifically down-regulate GFP protein expression. The cells were incubated for 72 hours with the different carriers containing 10 to 50 nM of siRNA per well before removing them using trypsin. For statistical analysis, the level of GFP expression was determined by flow cytometry analysis on a FACScalibur flow cytometer (BD Bioscience). Cells that do not express GFP were used to calibrate flow cytometer. As a nonspecific control, siRNA that has no homology to any known mammalian gene was used for transfection with the different nanocarriers. At least 10^4 events were collected and analyzed using the WinMDI 2.9 software.

2.7. Cytotoxicity

Cell viability was measured through the net metabolic activity using a colorimetric assay for 96-well plates with 2-(4-iodophenyl)-3-(4-nitrophenyl)-5-(2,4-disulfophenyl)-2H-tetrazolium monosodium salt (WST-1) reagent (Roche, France). MDA-MB231 cells were seeded at 4.10^4 cells/well (0.2 mL per well) and allowed to grow 24 h in an incubator in standard cell culture conditions. On the day of the experiment, different concentrations of siRNA (from 1 to 100 nM) included in S-MSN were incubated with the cells for 24 h. Then, the culture medium was removed and fresh complete medium without phenol red was added for further 24 h incubation. 10% WST-1 reagent was added to the culture medium and kept in the incubator for 3 hours. Cells without S-MSN were used as negative controls whereas cells incubated with H_2O_2 (20 mM) were used as positive controls. Absorbance was recorded at 450 nm (to detect the reaction product formazan) and 690 nm (background subtraction) using a microplate reader. The absorbance difference ($A_{450nm} - A_{690nm}$) was directly proportional to the number of viable cells and the percentage cell viability was determined using the following equation: Viability (%) = $(A_S\text{-}A_{PC})/(A_{NC}\text{-}A_{PC}) \times 100$; where A_S, A_{PC} and A_{NC} represent absorbances of the sample, the positive control and negative control respectively.

2.8. Statistical analysis

Data are expressed as mean ± SD of the variables and are compared among groups by using one-way ANOVA followed by Fisher's protected Least Significance Difference test.

3. Results

3.1. From MSN to S-MSN: Stealth fluorescent particles (SFP) as precursors

MSN suspensions in aqueous buffers have a HD of 70 nm (intensity average) and a ZP of +20 mV (Table 1), similarly to previously reported studies (David et al., 2015, 2013). Compared to initial aminosilane treated SPIONs, MSN coated with siRNA and chitosan have an increased HD (+23 nm), but nearly the same ZP (Table 1). Incubation of MSN in complete cell culture medium containing 5% fetal calf serum at 37 °C triggered a large increase of their hydrodynamic diameter over time (data not shown). Thus, in the presence of serum proteins, MSN did not assure an appropriate colloidal stability.

Prior to S-MSN formulations, aminated SPIONs were covalently labeled with sulfocyanine and coated with PEG 5 kDa (Alric et al.,

Table 1
Physico-chemical characterization of MSN and S-MSN: S-MSN_1 contained SFP, chitosan and siRNA; S-MSN_2 were formulated with SFP, PLR and siRNA, whereas S-MSN_3 were optimized with both cationic polymers chitosan and PLR. Measures were performed with siRNA concentrations of 20 nM in $NaNO_3$ 0.01 M by dynamic light scattering on Malvern ZetaSizer. Conductivity was constant between 1.1 and 1.2 mS/cm (n = 3).

	Hydrodynamic diameter (HD) *nm*	Polydispersity (PDI)	Zeta potential (ZP) *mV*
Spion *PEG−/sulfocyanine−*	47 ± 4	0.15 ± 0.03	22 ± 5
SFP *PEG+/sulfocyanine+*	60 ± 3	0.16 ± 0.02	2 ± 3
MSN *with Spion*	70 ± 6	0.27 ± 0.05	20 ± 5
S-MSN_1 *with SFP*	76 ± 4	0.25 ± 0.03	12 ± 2
S-MSN_2 *with SFP*	61 ± 3	0.22 ± 0.02	3 ± 1
S-MSN_3 *with SFP*	64 ± 3	0.17 ± 0.03	5 ± 1

2016; Perillo et al., 2017), to generate SFP. At a hydrodynamic diameter of about 60 nm, the SFP are bigger than SPIONs, which is consistent with the presence of the PEG coating around nanoparticles. Moreover, the PEG shell apparently hides the positive charges of aminosilanes, reducing the ZP to close to neutral charge (Table 1).

3.1.1. Protocol 1 (synthesis of S-MSN_1): replacement of SPIONs by SFP to increase the colloidal stability

The S-MSN_1 were generated by loading SFP with a mixture of siRNA (50 nM) and chitosan (CR_{CS} = 44) in DPBS 1 × buffer. The HD and ZP of S-MSN_1 were 76 nm and 12 mV (Table 1). Thus, the addition of chitosan and siRNA led to an increase in HD (+ 16 nm) and ZP (+ 10 mV) (Table 1). Compared to MSN, the S-MSN_1 have a slightly bigger HD, as well as lower polydispersity and ZP (Table 1). These values are consistent with the presence of a PEG layer in S-MSN_1. In contrast to MSN of the same CR_{CS} (= 44) and MR (= 10), S-MSN_1 suspensions were colloidally stable for at least 4 hours of incubation in a serum-containing cell culture medium at 37 °C (Fig. 1A). In such conditions, S-MSN_1 displayed an increase of hydrodynamic diameter (about 40 nm after incubation with cell culture medium), then remained stable whatever the tested incubation duration. In this study, a minor population was observed around 13 nm in every incubation time: this population represents serum proteins from culture medium (Fig. 1A). The polydispersity, however, decreases significantly over four hours, probably due to the higher ionic strength in culture media.

Despite a better colloidal stability in culture medium, complexation with S-MSN_1 was not completely effective (Fig. 1B). A gel retardation assay was performed in order to determine the amount of siRNA complexed on S-MSN_1: compared to the condition with heparin allowing a complete siRNA release, about 75% siRNA were complexed within S-MSN_1 (Fig. 1B). This lack of complexation was coherent with the results obtained for the complexation between chitosan and siRNA (Fig. 1B).

In order to study transfection efficiency, MDA-MB231-GFP cells are used that normally produce a fluorescent protein GFP. The fluorescence intensity of individual cells is measured by flow cytometry, and the number of cells displaying a certain fluorescence intensity is plotted as a function of intensity (Supplementary data Fig. 1A). When cells, incubated for 72 hours with S-MSN_1 carrying 20 nM siRNA are analyzed, a practically identical profile with untreated cells is obtained, which proves that no transfection occurred with these nanocarriers. Either the nanoparticles do not penetrate into the cells or the siRNA is released prematurely. In order to improve complexation we tried to immobilize the siRNA with a different cationic polymer in our second protocol.

3.1.2. Protocol 2 (synthesis of S-MSN_2): replacement of chitosan with PLR to increase complexation

In the formulation of S-MSN_2, we proceeded first to a complexation of anionic siRNA with cationic PLR, which possesses a significantly higher cationic charge than chitosan at physiologically relevant pH and should thus enhance transfection efficiency (Ragelle et al., 2013). The pre-formed siRNA-PLR molecular complex was then incubated with SFP. The optimal quantity of PLR was determined through its ability to prevent the release of siRNA from nanocarriers during a gel retardation assay (Fig. 2). For a constant amount of siRNA and SFP (MR = 10), the charge ratio between PLR and siRNA (CR_{PS}) was increased from 1 to 44. Concentration of free siRNA diminished with increasing CR_{PS}: compared to a control, only 0.2% of siRNA was released with a CR_{PS} of 24. From CR_{PS} of 28, the totality of the loaded siRNA remained on S-MSN (Fig. 2).

Compared to S-MSN_1, the hydrodynamic diameter of the optimized charge ratio (CR = 28) S-MSN_2 was 15 nm smaller (Table 1). This difference was probably due to the PLR molecules that may produce a more compact complex with siRNA, in line with the lower polydispersity (Table 1). Unexpectedly, the zeta potential of S-MSN_2 was around 3 mV, i.e. 3.7 times lower than that of S-MSN_1 and close to that of SFP (Table 1). The siRNA-PLR complex compaction into S-MSN_2 could enable more efficient shielding of the siRNA-PLR charges within the PEG coating.

Despite a better complexation with these optimized S-MSN_2 (MR = 10 and CR_{PS} = 28), GFP expression was not significantly down-regulated after 20 nM siRNA transfection (Supplementary data Fig. 1B). Therefore, a third protocol of the S-MSN formulation has been developed and described below.

3.1.3. Protocol 3 (synthesis of S-MSN_3): loading of siRNA together with both PLR and chitosan to reach the transfection efficiency of commercially available transfection reagent Oligofectamine®

From the previous experiments, S-MSN_3 was developed. The protocol comprised the siRNA/PLR pre-complexation prior to adding them to a mixture of SFP and chitosan. According to previous protocols, the initial formulation of S-MSN_3 was characterized by MR of 10, CR_{CS} of 44, and CR_{PS} of 28. In order to optimize the biological response, each of these three parameters was varied individually, maintaining the other two constant. The results of transfection with S-MSN_3 of different quantitative composition on MDA-MB231-GFP are shown in Fig. 3.

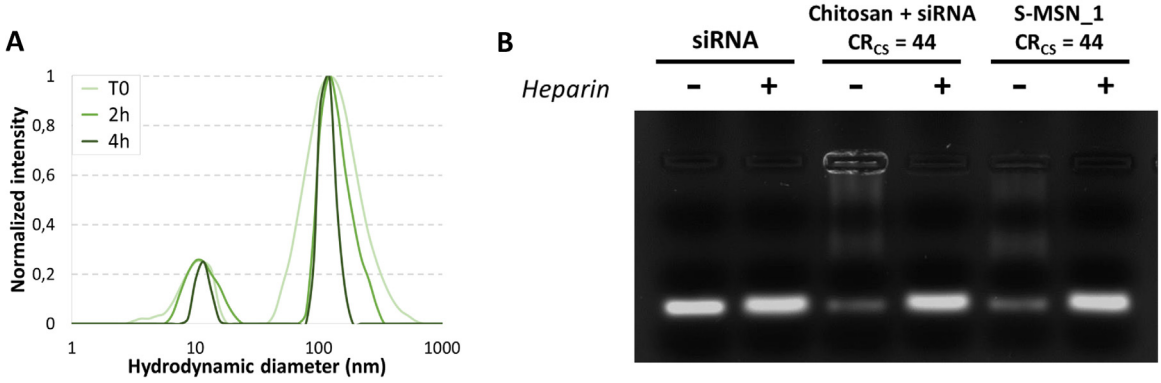

Fig. 1. S-MSN_1. (A) Stability in culture media. S-MSN_1 containing siRNA (20 nM), SFP (MR = 10) and chitosan (CR_{CS} = 44) were studied for colloidal stability in complete culture medium through dynamic light scattering (n = 3). (B) Complexation. Gel retardation assay on chitosan-siRNA polyplex and S-MSN_1 with a constant concentration of siRNA (3 μM) and CR_{CS} (44).

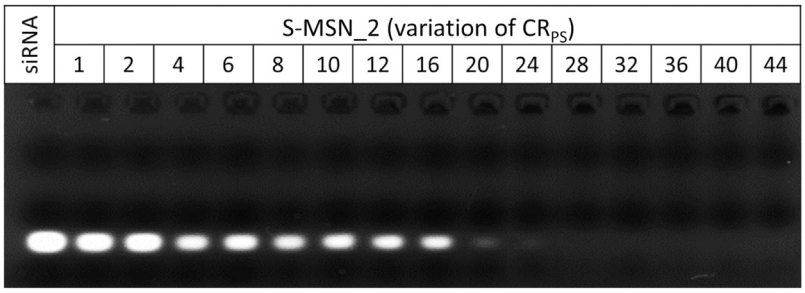

Fig. 2. S-MSN_2. Complexation. Gel retardation assay on S-MSN_2 with a constant concentration of siRNA (3 μM) and CR_{PS} varying from 1 to 44.

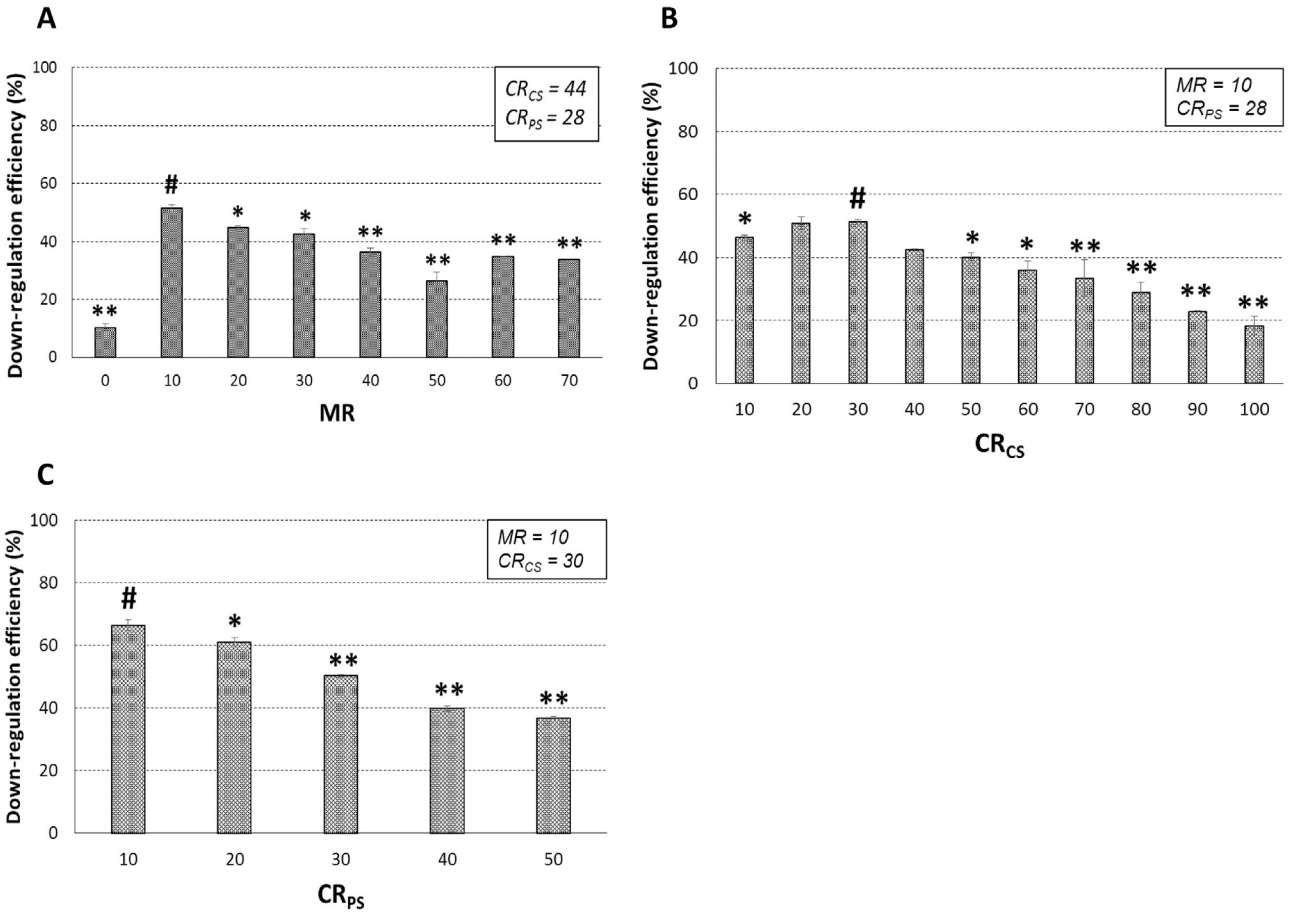

Fig. 3. Optimization of S-MSN_3 for down-regulation efficiency: Fluorescence intensity of MDA-MB231/GFP after 72 hours incubation with 0.13 μg siRNA-GFP included into S-MSN_3. Different components were optimized: (A) MR (B) CR_{CS} and (C) CR_{PS}. #: reference value for statistics; *: $p < 0.05$; **: $p < 0.01$ (mean +/− SD, n = 6).

(i) With a constant siRNA quantity (10 nmol), CR_{CS} (= 44) and CR_{PS} (= 28), the quantity of SPION was adjusted according to a MR from 10 to 70 (Fig. 3A). A control condition of chitosan-PLR-siRNA polyplexes (MR = 0) demonstrated a major contribution of SPION for functional siRNA transfection as this condition led to low GFP down-regulation efficiency (10.3%). However, an increase in SPION concentration (MR ≥ 10) was correlated with a lowered GFP down-regulation efficiency, from 52.3% to 28.6% (Fig. 3A). Thus, a MR of 10 was chosen as the optimal formulation condition for further experiments.

(ii) With fixed MR (= 10), CR_{PS} (= 28) and siRNA quantity (10 nmol), the chitosan concentration was varied corresponding to a CR_{CS} from 10 to 100 (Fig. 3B). Up to a CR_{CS} of 30, GFP down-regulation efficiency increased with the amount of chitosan, reaching a maximum of around 52% (Fig. 3B). For higher chitosan content, the GFP down-regulation was less pronounced (Fig. 3B), demonstrating the impact of chitosan on siRNA transfection. The optimal amount of chitosan used for further experiments was considered to be a CR_{CS} of 30.

(iii) With fixed MR (= 10), CR_{CS} (= 30) and siRNA quantity (10 nmol), the CR_{PS} was varied from 10 to 50 (Fig. 3C). Unexpectedly, GFP down-regulation efficiency was directly reduced with the increase of PLR (Fig. 3C), showing the need to reduce CR_{PS} to 10 in order to obtain optimal results. Compared to results obtained with CR_{PS} at 30 (Fig. 3C), GFP down-regulation was improved up to 67% with optimum balance between the various components. CR_{PS} of 10 was chosen as optimal formulation condition for further experiments.

(iv) With optimal data defined previously (CR_{CS} = 30; CR_{PS} = 10; MR = 10), the concentration of siRNA incorporated into the

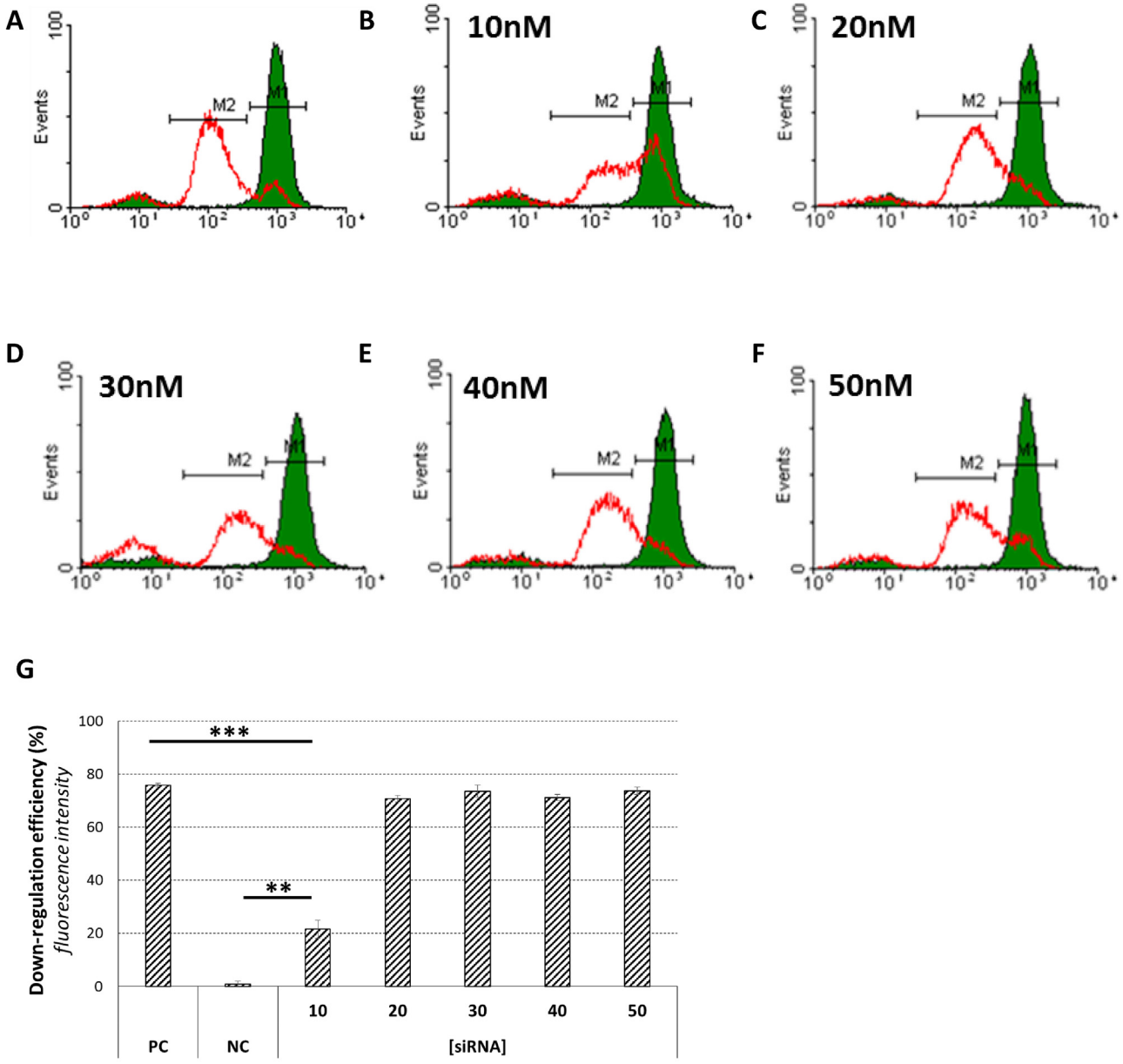

Fig. 4. Optimization of siRNA concentration with S-MSN_3 for down-regulation efficiency. Fluorescence intensity of MDA-MB231/GFP cells after 72 hours transfection with (A) Positive control (PC): transfection with commercially available reagent Oligofectamine® (20 nM siGFP). (B – F) S-MSN_3 with different siGFP concentrations (10, 20, 30, 40 and 50 nM for B, C, D, E, F, respectively). (G) Down-regulation efficiencies (conditions (A – F)) represented as decrease in fluorescence intensity. S-MSN_3 formulation with negative control siRNA (NC) was assessed at 20 nM. Green spectra with a black line represent MDA-MB231/GFP cells without transfection, whereas red line spectra are obtained after S-MSN_3 or Oligofectamine® transfection. ***: $p < 0.001$ (mean +/– SD, n = 3). For interpretation of the references to color in this figure legend, the reader is referred to the web version of the article.

formulation of S-MSN_3 was also varied from 10 nM to 50 nM (Fig. 4). The fluorescence intensity of individual cells is measured by flow cytometry, and the number of cells displaying a certain fluorescence intensity is plotted as a function of intensity. For non-transfected cells, the green curve is obtained showing a relatively homogeneous population of fluorescing cells (at about 10^3 units). A sub-population of particles with a 100-fold lower fluorescence intensity is also observed that corresponds to cellular debris and/or cells that do not express GFP protein. After successful transfection, the expression of GFP should be down-regulated, leading to cells with a lower fluorescence intensity (the main peak in the graph should be shifted to the left). For all siRNA concentrations above 20 nM (Fig. 4C), the peak of fluorescence intensity is shifted to about $2 \cdot 10^2$ units, which means that GFP content in most cells has decreased by a factor of 5: high specific GFP down-regulation was observed with 71% decrease in fluorescence intensity compared to negative control (NC) (Fig. 4G). S-MSN_3 containing from 20 to 50 nM siRNA showed comparable down-regulation efficiency displaying high ability to carry active siRNA. However, S-MSN_3 with only 10 nM siRNA reduced the down-regulation efficiency by a factor of 3 (Fig. 4B and G).

Compared to S-MSN_3, the commercially available reagent Oligofectamine® displayed a similar GFP down-regulation efficiency (Fig. 4A and G). The main difference was in the GFP distribution: with this commercial lipoplex, two distinct populations appeared, cells with or without GFP (Fig. 4A). On the contrary, with S-MSN_3 at 20 nM siRNA concentration, only one cell population with homogeneous GFP expression was observed

(Fig. 4C). With higher siRNA concentration of 50 nM (Fig. 4F), the GFP expression profile was significantly close to Oligofectamine®: 20 nM siRNA was therefore considered as optimum with S-MSN_3.

3.2. Safety, retention and protection required for in vivo adaptation of optimized S-MSN formulation

Among the features required for these nanocarriers with a view to *in vivo* adaptation, low S-MSN cytotoxicity as well as high siRNA retention and protection have to be provided. Cytotoxicity was assessed via the mitochondrial activity reduction depending on siRNA concentration in S-MSN_3 (Fig. 5). In 24 hours incubation with S-MSN_3, their cytotoxic effects seemed to be limited up to a siRNA concentration of 100 nM where cell viability remained as high as 87% (Fig. 5). This high safety could allow the increase of S-MSN_3 concentrations for certain conditions such as hard-to-transfect cells.

Complexation of siRNA with optimal S-MSN_3 formulation was assessed through gel retardation assay (supplementary data Fig. 2): no siRNA release was observed for S-MSN_3, displaying that all siRNA used for the formulation were complexed within S-MSN_3. In the same way, the siRNA retention in S-MSN incubated for various duration in a cell culture medium containing 5% fetal calf serum at 37 °C was monitored using a gel retardation assay (Fig. 6A). For each condition, a control with 10 mg/mL heparin was used in order to release siRNA. Immediately after the contact with the complete culture medium, less than 7% of siRNA had been released (Fig. 6A) and no additional release was observable till 4 hours demonstrating a high retention by S-MSN_3. Even by increasing the amount of fetal calf serum to 50%, the siRNA integrity remained significant (60-70%), with 80% of non-degraded siRNA retained in S-MSN_3 after 4 hours incubation (Supplementary data Fig. 3).

These results was consistent with the siRNA protection against ribonuclease A (Fig. 6B). While free siRNA was totally degraded after 30 minutes of incubation with the enzyme, S-MSN_3 protected siRNA even after 4 hours. More than 90% of siRNA kept their integrity upon the siRNA release stimulated using heparin sodium (Fig. 6B).

4. Discussion

S-MSN_1 have demonstrated promising results concerning their colloidal stability and complexation with siRNA. However, the use of chitosan as unique cationic polymer in the formulation did not allow reaching an efficient GFP down-regulation in MDA-MB231-GFP cells treated with the S-MSN_1 (Fig. 1). Similar limitations of chitosan as agent for *in vitro* and *in vivo* siRNA transfection have been previously described (Mao et al., 2001; Ragelle et al., 2013). Indeed, each deacetylated subunit of chitosan contains a primary amine group with a pKa value of about 6.5. S-MSN formulation occurred at a pH below the chitosan pKa enabling efficient complexation: at pH 5.5-5.7, about 90% of the amino groups were protonated (Mao et al., 2001). However, pH increase to 7.2-7.4 in the cell culture media may reduce the cationic nature of chitosan (Mao et al., 2001). Nevertheless, the role of chitosan remains essential during siRNA transfection to cells *in vitro*, probably for endosomal escape in order to reach cytoplasmic compartment after internalization through vesicles. In such cases, within the acidic endosomal environment, the protonation of chitosan amine groups results to an increased influx of Cl^- ions and water: the combination of the osmotic swelling (called proton-sponge effect) and a swelling of the chitosan because of repulsion between protonated amine groups (called umbrella effect) causes the rupture of the lysosomal membrane with subsequent release of its contents into the cytoplasm (Nguyen and Szoka, 2012).

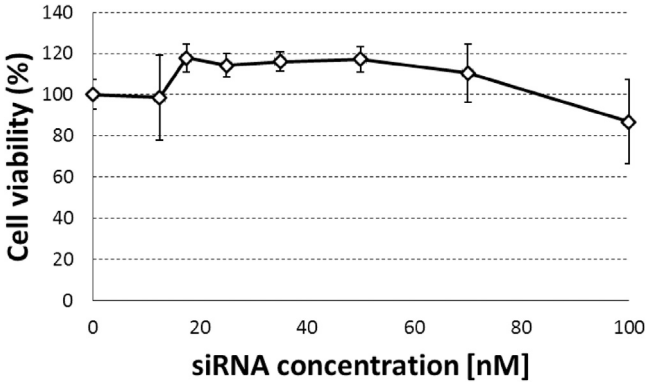

Fig. 5. Cytotoxicity assay on breast cancer cells MDA-MB231 with S-MSN_3. Metabolic activity from WST-1 assay after 24 hours incubation at different siRNA concentrations (with $CR_{CS} = 30$, $CR_{PS} = 10$ and MR = 10) (mean +/− SD, n = 6).

Addition of other cationic polymers represents an interesting approach to overcome the chitosan-related limitation described above. For example, poly-ethylene imine (PEI) (Akinc et al., 2005) and PLR (Kim et al., 2009; Veiseh et al., 2011) have been used in combination with chitosan to promote siRNA transfection. After PEI grafting onto chitosan using an imine reaction, these polymers allowed 55% silencing of GFP expression on adenocarcinomic human alveolar basal epithelial cells A549 after transfection with 50 nM siRNA (Jere et al., 2009). Nevertheless, PEI is generally described to exhibit significant *in vitro* and *in vivo* toxicity in addition to a lack of stability (Merkel et al., 2009). Another polymer, poly-L-arginine (PLR) and its derivatives, seems to be more promising and was shown to lead to the effective down-regulation of targeted genes on different cell lines (Noh et al., 2010). The pKa of PLR is about 12, which favors its cationic nature and its electrostatic interactions with siRNA at physiological pH. In our study, addition of PLR to siRNA and chitosan ($CR_{CS} = 30$) provided a large improvement of GFP down-regulation efficiency when used at a charge ratio CR_{PS} of 10 (Fig. 3).

However, with a larger excess of PLR ($CR_{PS} > 10$), the GFP silencing activity diminished (Fig. 3C). This could be explained with two hypothesis: (1) the strong interaction between PLR and siRNA prevents them from being delivered into cytoplasmic compartment and limits their RISC accessibility. (2) Following the protocol, the pre-complex siRNA/PLR was added to a solution of SPION/Chitosan. Also, during formulation, PLR/siRNA could trap low-charged chitosan on the SFP: this is observable with hydrodynamic diameter comparison between S-MSN_1 and S-MSN_3. Without PLR, S-MSN_1 displayed 76 nm whereas the compaction allowed by PLR in S-MSN_3 led to a hydrodynamic diameter of 63 nm, even with chitosan presence (Table 1). In this hypothesis, when the acidification of the endosome enables the protonation of chitosan amine groups, the electrostatic repulsion between cationic charges triggers polymer expansion and umbrella effect (Nguyen and Szoka, 2012). With a too strong interaction between PLR and siRNA, this effect could be reduced, diminishing endosomal escape and siRNA release into cytoplasm (Fig. 3C).

The optimization of different formulation parameters and the comprehension of their interaction enable to achieve 70% gene silencing efficiency on MDA-MB231-GFP cells using S-MSN_3 (see the flow cytometry data in Figs. 3 and 4). This efficiency was close to that of commercially available lipoplexe Oligofectamine® (Fig. 4). Previous studies have already reported the efficient siRNA transfection by SPION combined to chitosan and other molecules: with linoleic acid, Cheong et al. demonstrated strong down-regulation of GFP in hepatocytes (Cheong et al., 2009). However, nature of molecules associated to inorganic nanoparticles remains

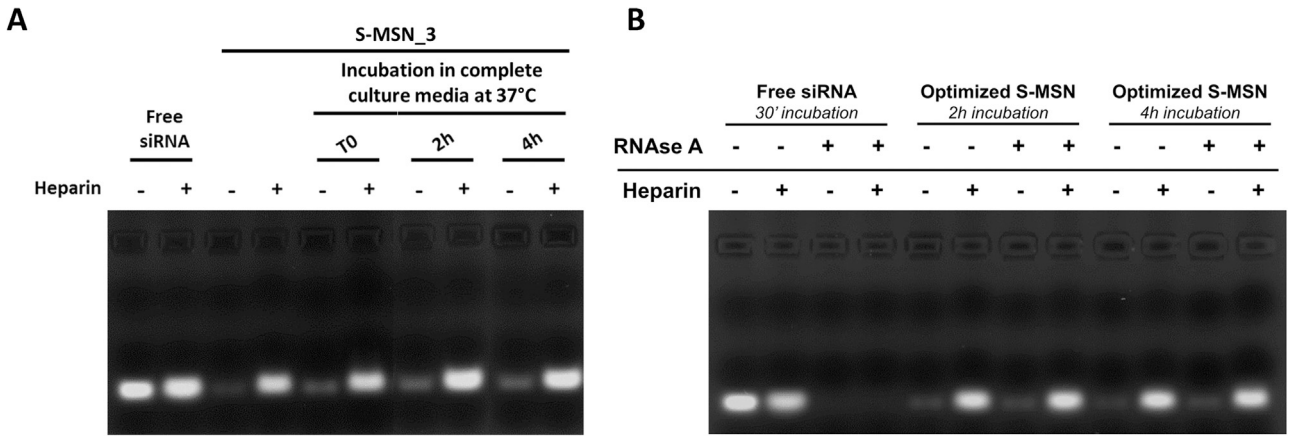

Fig. 6. Protection and retention of siRNA on S-MSN_3. Gel retardation assay with constant concentration of S-MSN_3 ([siRNA] 3 μM) after incubation from 0 to 4 h (A) in complete culture medium or (B) with ribonuclease A (400 ng/mL). Heparin sodium (10 μg/mL) was used to release siRNA from S-MSN complex as a control condition.

a key issue, especially for internalization and endosomal escape. Many studies have shown weak silencing activity attributed to a major accumulation of nanocarriers in endosomes (Ding et al., 2014; Perche et al., 2016; Wu et al., 2014) and required strategies to overcome this limitation, such as endosomal escape enhancer (Perche et al., 2016). Thus, Perche et al. had shown that transfection with high siRNA concentration (up to 200 nM) resulted in a down-regulation efficiency close to that obtained with commercially available lipoplexes (Perche et al., 2016). Our results demonstrate that S-MSN_3 favor siRNA transfection into cytoplasm of cancer cells and results in a strong down-regulation of targeted gene, even at concentration of 20 nM (Fig. 5).

Efficient siRNA nanocarriers have to protect siRNA against degradation from enzymes such as ribonucleases. Moreover, siRNA release need to be avoided until they reach targeted cells or tissues. In the literature, inorganic nanoparticles modified with positively charged L-arginine have already been reported to provide effective protection of siRNA from enzymatic degradation (Li et al., 2011). Besides, other molecules used in formulation could induce some steric hindrance limiting siRNA accessibility to RNAses (Li et al., 2011). With S-MSN_3, chitosan and PLR prevent siRNA from degradation even after several hours of incubation with RNAse A (Fig. 6B). Furthermore, the S-MSN_3 prevented siRNA release in culture media containing fetal bovine serum (Fig. 6A). These results could be explained through a better compaction of siRNA/PLR onto SFP allowing protection by PEG. Nevertheless, a balance between protection and release of siRNA is required to allow the siRNA to act in the cellular cytoplasm. Excessive siRNA protection may hinder their endosomal escape and result in its total degradation into lysosome (Zeller et al., 2015). S-MSN_3 appear to be in line with all the necessary requirements since the down-regulation of the targeted gene was observed after siRNA transfection (Fig. 4).

5. Conclusion

In this study, stealth magnetic siRNA nanocarriers S-MSN_3 were able to provide effective siRNA transfection to the cytosol of breast cancer cells MDA-MB231. Down-regulation of GFP protein by transfected siRNA was confirmed by strong reduction of cytosolic fluorescence intensity. According to their size below 100 nm, nearly neutral surface and their ability to protect siRNA from enzymatic degradation, the S-MSN_3 appear as promising nanomedicine form. In the close future, we will start their evaluation *in vivo*. In parallel, we will advance this nanomedicine form with antibody fragments grafted onto the PEG shell, for active and specific targeting of breast cancer cells.

Acknowledgments

This work is supported by the “Institut National du Cancer (INCa)”, the “Fondation ARC” and the “Ligue Nationale Contre le Cancer (LNCC)” (ARC_INCa_LNCC_7636). We are thankful to the "Région Centre-Val de Loire" (NCIS Project). The authors would like to thank Isabelle Dimier-Poisson and Nathalie Moire (UMR INRA 1282, team of “Infectiologie et Santé Publique”, University François Rabelais of Tours) for her help with flow cytometry experiments and Didier Bedin (EA6295, "Nanomédicaments et nanosondes", University François Rabelais of Tours) for technical support.

Appendix A. Supplementary data

Supplementary data associated with this article can be found, in the online version, at http://dx.doi.org/10.1016/j.ijpharm.2017.05.022.

References

Akinc, A., Thomas, M., Klibanov, A.M., Langer, R., 2005. Exploring polyethylenimine-mediated DNA transfection and the proton sponge hypothesis. J. Gene Med. 7, 657–663. doi:http://dx.doi.org/10.1002/jgm.696.

Alric, C., Aubrey, N., Allard-Vannier, E., di Tommaso, A., Blondy, T., Dimier-Poisson, I., Chourpa, I., Hervé-Aubert, K., 2016. Covalent conjugation of cysteine-engineered scFv to PEGylated magnetic nanoprobes for immunotargeting of breast cancer cells. RSC Adv . 6, 37099. doi:http://dx.doi.org/10.1039/c6ra06076e.

Cheong, S.J., Lee, C.M., Kim, S.L., Jeong, H.J., Kim, E.M., Park, E.H., Kim, D.W., Lim, S.T., Sohn, M.H., 2009. Superparamagnetic iron oxide nanoparticles-loaded chitosan-linoleic acid nanoparticles as an effective hepatocyte-targeted gene delivery system. Int. J. Pharm. 372, 169–176. doi:http://dx.doi.org/10.1016/j.ijpharm.2009.01.009.

David, S., Marchais, H., Bedin, D., Chourpa, I., 2015. Modelling the response surface to predict the hydrodynamic diameters of theranostic magnetic siRNA nanovectors. Int. J. Pharm. 478, 409–415. doi:http://dx.doi.org/10.1016/j.ijpharm.2014.11.061.

David, S., Marchais, H., Hervé-Aubert, K., Bedin, D., Garin, A.-S., Hoinard, C., Chourpa, I., 2013. Use of experimental design methodology for the development of new magnetic siRNA nanovectors (MSN). Int. J. Pharm. 454, 660–667. doi:http://dx.doi.org/10.1016/j.ijpharm.2013.05.051.

De Fougerolles, A., Novobrantseva, T., 2008. siRNA and the lung: research tool or therapeutic drug? Curr. Curr. Opin. Pharmacol. 8, 280–285. doi:http://dx.doi.org/10.1016/j.coph.2008.04.005.

Ding, Y., Jiang, Z., Saha, K., Kim, C.S., Kim, S.T., Landis, R.F., Rotello, V.M., 2014. Gold nanoparticles for nucleic acid delivery. Mol. Ther. 22, 1075–1083. doi:http://dx.doi.org/10.1038/mt.2014.30.

Ferlay, J., Soerjomataram, I., Dikshit, R., Eser, S., Mathers, C., Rebelo, M., Parkin, D.M., Forman, D., Bray, F., 2015. Cancer incidence and mortality worldwide: Sources, methods and major patterns in GLOBOCAN 2012. Int. J. Cancer 136, E359–E386. doi:http://dx.doi.org/10.1002/ijc.29210.

Fire, A., Xu, S., Montgomery, M.K., Kostas, S.A., Driver, S.E., Mello, C.C., 1998. Potent and specific genetic interference by double-stranded RNA in Caenorhabditis elegans. Nature 391, 806–811. doi:http://dx.doi.org/10.1038/35888.

Howard, K.A., Rahbek, U.L., Liu, X., Damgaard, C.K., Glud, S.Z., Andersen, M.Ø., Hovgaard, M.B., Schmitz, A., Nyengaard, J.R., Besenbacher, F., Kjems, J., 2006. RNA interference in vitro and in vivo using a novel chitosan/siRNA nanoparticle system. Mol. Ther. 14, 476–484. doi:http://dx.doi.org/10.1016/j.ymthe.2006.04.010.

Jere, D., Jiang, H.-L., Kim, Y.-K., Arote, R., Choi, Y.-J., Yun, C.-H., Cho, M.-H., Cho, C.-S., 2009. Chitosan-graft-polyethylenimine for Akt1 siRNA delivery to lung cancer cells. Int. J. Pharm. 378, 194–200. doi:http://dx.doi.org/10.1016/j.ijpharm.2009.05.046.

Juliano, R., Alam, M.R., Dixit, V., Kang, H., 2008. Mechanisms and strategies for effective delivery of antisense and siRNA oligonucleotides. Nucleic Acids Res. 36, 4158–4171. doi:http://dx.doi.org/10.1093/nar/gkn342.

Kennecke, H., Yerushalmi, R., Woods, R., Cheang, M.C.U., Voduc, D., Speers, C.H., Nielsen, T.O., Gelmon, K., 2010. Metastatic behavior of breast cancer subtypes. J. Clin. Oncol. 28, 3271–3277. doi:http://dx.doi.org/10.1200/JCO.2009.25.9820.

Kim, E.-J., Shim, G., Kim, K., Kwon, I.C., Oh, Y.-K., Shim, C.-K., 2009. Hyaluronic acid complexed to biodegradable poly L-arginine for targeted delivery of siRNAs. J. Gene. Med. 11, 791–803. doi:http://dx.doi.org/10.1002/jgm.1352.

Lavertu, M., Méthot, S., Tran-Khanh, N., Buschmann, M.D., 2006. High efficiency gene transfer using chitosan/DNA nanoparticles with specific combinations of molecular weight and degree of deacetylation. Biomaterials 27, 4815–4824. doi:http://dx.doi.org/10.1016/j.biomaterials.2006.04.029.

Layzer, J.M., McCaffrey, A.P., Tanner, A.K., Huang, Z., Kay, M.A., Sullenger, B.A., 2004. In vivo activity of nuclease-resistant siRNAs. RNA 10, 766–771. doi:http://dx.doi.org/10.1261/RNA.5239604.

Li, J.M., Zhao, M.X., Su, H., Wang, Y.Y., Tan, C.P., Ji, L.N., Mao, Z.W., 2011. Multifunctional quantum-dot-based siRNA delivery for HPV18 E6 gene silence and intracellular imaging. Biomaterials 32, 7978–7987. doi:http://dx.doi.org/10.1016/j.biomaterials.2011.07.011.

Mao, H.Q., Roy, K., Troung-Le, V.L., Janes, K. a., Lin, K.Y., Wang, Y., August, J.T., Leong, K.W., 2001. Chitosan-DNA nanoparticles as gene carriers: Synthesis, characterization and transfection efficiency. J. Control. Release 70, 399–421. doi:http://dx.doi.org/10.1016/S0168-3659(00)00361-8.

Mao, S., Sun, W., Kissel, T., 2010. Chitosan-based formulations for delivery of DNA and siRNA. Adv. Drug Deliv. Rev. 62, 12–27. doi:http://dx.doi.org/10.1016/j.addr.2009.08.004.

Medarova, Z., Pham, W., Farrar, C., Petkova, V., Moore, A., 2007. In vivo imaging of siRNA delivery and silencing in tumors. Nat. med 13, 372–377. doi:http://dx.doi.org/10.1038/nm1486.

Meister, G., Tuschl, T., 2004. Mechanisms of gene silencing by double-stranded RNA. Nature 431, 343–349. doi:http://dx.doi.org/10.1038/nature02873.

Merkel, O.M., Librizzi, D., Pfestroff, A., Schurrat, T., Buyens, K., Sanders, N.N., De Smedt, S.C., Behe, M., Kissel, T., 2009. Stability of siRNA polyplexes from poly(ethylenimine) and poly(ethylenimine)-g-poly(ethylene glycol) under in vivo conditions: effects on pharmacokinetics and biodistribution measured by luorescence Fluctuation Spectroscopy and Single Photon Emission Computed Tomography (SPECT) imaging. J. Control. Release. 138, 148–159. doi:http://dx.doi.org/10.1016/j.jconrel.2009.05.01.

Nguyen, J., Szoka, F.C., 2012. Nucleic acid delivery: the missing pieces of the puzzle? Acc. Chem. Res. 45, 1153–1162. doi:http://dx.doi.org/10.1021/ar3000162.

Noh, S.M., Park, M.O., Shim, G., Han, S.E., Lee, H.Y., Huh, J.H., Kim, M.S., Choi, J.J., Kim, K., Kwon, I.C., Kim, J.-S., Baek, K.-H., Oh, Y.-K., 2010. Pegylated poly-l-arginine derivatives of chitosan for effective delivery of siRNA. J. Control. Release 145, 159–164. doi:http://dx.doi.org/10.1016/j.jconrel.2010.04.005.

Opanasopit, P., Tragulpakseerojn, J., Apirakaramwong, A., Ngawhirunpat, T., Rojanarata, T., 2011. Chitosan enhances transfection efficiency of cationic polypeptides/DNA complexes. Int. J. Pharm. 410, 161–168. doi:http://dx.doi.org/10.1016/j.ijpharm.2011.03.008.

Ozcan, G., Ozpolat, B., Coleman, R.L., Sood, A.K., Lopez-Berestein, G., 2015. Preclinical and clinical development of siRNA-based therapeutics. Adv. Drug Deliv. Rev. 87, 108–119. doi:http://dx.doi.org/10.1016/j.addr.2015.01.007.

Perche, F., Yi, Y., Hespel, L., Mi, P., Dirisala, a., Cabral, H., Miyata, K., Kataoka, K., 2016. Hydroxychloroquine-conjugated gold nanoparticles for improved siRNA activity. Biomaterials 90, 62–71. doi:http://dx.doi.org/10.1016/j.biomaterials.2016.02.027.

Perillo, E., Hervé-Aubert, K., Allard-Vannier, E., Falanga, A., Galdiero, S., Chourpa, I., 2017. Synthesis and in vitro evaluation of fluorescent and magnetic nanoparticles functionnalized with a cell penetrating peptide for cancer theranosis. J. Colloid Interface Sci. 499, 209–217. doi:http://dx.doi.org/10.1016/j.jcis.2017.03.106.

Ragelle, H., Vandermeulen, G., Préat, V., 2013. Chitosan-based siRNA delivery systems. J. Control Release 172, 207–218. doi:http://dx.doi.org/10.1016/j.jconrel.2013.08.005.

Resnier, P., Montier, T., Mathieu, V., Benoit, J.P., Passirani, C., 2013. A review of the current status of siRNA nanomedicines in the treatment of cancer. Biomaterials 34, 6429–6443. doi:http://dx.doi.org/10.1016/j.biomaterials.2013.04.060.

Santel, a, Aleku, M., Keil, O., Endruschat, J., Esche, V., Fisch, G., Dames, S., Löffler, K., Fechtner, M., Arnold, W., Giese, K., Klippel, a, Kaufmann, J., 2006. A novel siRNA-lipoplex technology for RNA interference in the mouse vascular endothelium. Gene Ther. 13, 1222–1234. doi:http://dx.doi.org/10.1038/sj.gt.3302777.

Schlabach, M.R., Luo, J., Solimini, N.L., Hu, G., Xu, Q., Li, M.Z., Zhao, Z., Smogorzewska, A., Sowa, M.E., Ang, X.L., Westbrook, T.F., Liang, A.C., Chang, K., Hackett, J.A., Harper, J.W., Hannon, G.J., Elledge, S.J., 2008. Cancer proliferation gene discovery through functional genomics. Science 319, 620–624. doi:http://dx.doi.org/10.1126/science.1149200.

Techaarpornkul, S., Wongkupasert, S., Opanasopit, P., Apirakaramwong, A., Nunthanid, J., Ruktanonchai, U., 2010. Chitosan-mediated siRNA delivery in vitro: effect of polymer molecular weight, concentration and salt forms. AAPS PharmSciTech 11, 64–72. doi:http://dx.doi.org/10.1208/s12249-009-9355-6.

Urban-Klein, B., Werth, S., Abuharbeid, S., Czubayko, F., Aigner, a, 2005. RNAi-mediated gene-targeting through systemic application of polyethylenimine (PEI)-complexed siRNA in vivo. Gene Ther. 12, 461–466. doi:http://dx.doi.org/10.1038/sj.gt.3302425.

Veiseh, O., Kievit, F.M., Mok, H., Ayesh, J., Clark, C., Fang, C., Leung, M., Arami, H., Park, J.O., Zhang, M., 2011. Cell transcytosing poly-arginine coated magnetic nanovector for safe and effective siRNA delivery. Biomaterials 32, 5717–5725. doi:http://dx.doi.org/10.1016/j.biomaterials.2011.04.039.

Veiseh, O., Gunn, J.W., Zhang, M., 2010. Design and fabrication of magnetic nanoparticles for targeted drug delivery and imaging. Adv. Drug Deliv. Rev. 62, 284–304. doi:http://dx.doi.org/10.1016/j.addr.2009.11.002.

Wood, L.D., Parsons, D.W., Jones, S., Lin, J., Sjöblom, T., Leary, R.J., Shen, D., Boca, S.M., Barber, T., Ptak, J., Silliman, N., Szabo, S., Dezso, Z., Ustyanksky, V., Nikolskaya, T., Nikolsky, Y., Karchin, R., Wilson, P.A., Kaminker, J.S., Zhang, Z., Croshaw, R., Willis, J., Dawson, D., Shipitsin, M., Willson, J.K., Sukumar, S., Polyak, K., Park, B.H., Pethiyagoda, C.L., Pant, P.V., Ballinger, D.G., Sparks, A.B., Hartigan, J., Smith, D.R., Suh, E., Papadopoulos, N., Buckhaults, P., Markowitz, S.D., Parmigiani, G., Kinzler, K.W., Velculescu, V.E., 2007. The genomic landscapes of human breast and colorectal cancers. Science. 318, 1108–1113. doi:http://dx.doi.org/10.1126/science.1145720.

Wu, X.A., Choi, C.H.J., Zhang, C., Hao, L., Mirkin, C.A., 2014. Intracellular Fate of Spherical Nucleic Acid Nanoparticle Conjugates. J. Am. Chem. Soc. 136, 7726–7733. doi:http://dx.doi.org/10.1021/ja503010a.

Yu, Y.H., Kim, E., Park, D.E., Shim, G., Lee, S., Kim, Y.B., Kim, C.-W., Oh, Y.-K., 2012. Cationic solid lipid nanoparticles for co-delivery of paclitaxel and siRNA. Eur. J. Pharm. Biopharm. 80, 268–273. doi:http://dx.doi.org/10.1016/j.ejpb.2011.11.002.

Zeller, S., Choi, C.S., Uchil, P.D., Ban, H.S., Siefert, A., Fahmy, T.M., Mothes, W., Lee, S.K., Kumar, P., 2015. Attachment of cell-binding ligands to arginine-rich cell-penetrating peptides enables cytosolic translocation of complexed sirna. Chem. Biol. 22, 50–62. doi:http://dx.doi.org/10.1016/j.chembiol.2014.11.009.

Zhang, J., Li, X., Huang, L., 2014. Non-viral nanocarriers for siRNA delivery in breast cancer. J. Control. Release 190, 440–450. doi:http://dx.doi.org/10.1016/j.jconrel.2014.05.037.